GYPSUM-FREE PORTLAND CEMENT, AN ALKALI-ACTIVATED MATERIAL SUITABLE FOR ACID CORROSION PROTECTION

Ali Allahverdi[1], František Škvára[2]
[1]College of Chemical Engineering
Iran University of Science and Technology
[2]Department of Glass, Ceramics, and Inorganic Binders
Institute of Chemical Technology, Czech Republic

Abstract. Investigation by scanning electron microscopy and X-ray energy dispersion measurements (X-ray line analyses) were performed on a number of 90-day corroded gypsum-free Portland cement and ordinary Portland cement paste specimens placed in nitric acid solutions of respective pH of 1, 2, and 3. The results obtained show that the hardened paste specimens of gypsum-free and ordinary Portland cements are corroded by exactly the same mechanism. The only difference between the two types of cement is the corrosion rate. The absence of crystalline formations, typical of hardened OPC paste, together with the high density and degree of dispersion of hydration products are responsible for a relatively higher acid resistance in gypsum-free Portland cement.

Keywords. *Gypsum-free Portland cement, Nitric acid, Corrosion*

1 Introduction

The deteriorating effect of acid media on cement-based constructions has become a worrying problem all over the world. These media generally occur as acid rains and mists, industrial and urban sewages, and acid ground-waters. The extent of attack depends not only on the type and concentration of the attacking acid, but also on the properties of the material including the type of cement used. The authors thoroughly discussed and reviewed the phenomenon of acid corrosion of hydrated cement-based materials [1], [2].

Emergence of new cements, e.g. gypsum-free Portland cement ″GFPC″, during the past decades necessitates detailed experimental work to investigate their durability in aggressive acid environments. The purpose of this work is to investigate and compare the response of hardened GFPC paste to nitric acid attack. GFPC can be described as a system of ground ordinary Portland cement clinker + an anion-active

surface-active agent with hydroxyl groups (ligninsulfonate, sulfonated lignin, and sulfonated polyphenolate) + a hydrolysable alkali metal salt (carbonate, bicarbonate, and silicate). The differences between GFPC and ordinary Portland cement ″OPC″ lie in the grinding (absence of gypsum and higher Blaine fineness in the range of 300 to 700 m^2/kg) and in the set regulator [3], [4]. The basic advantage of GFPC over OPC is the possibility of preparing paste, mortar, and concretes at considerably lower values of W/C [3]–[6].

The properties of GFPC are different from those of OPC. They display, for example, higher strength (≈100 MPa after 28 days of curing), durability, and thermal stability [3]–[8]. Hardened GFPC paste shows a low absorption capacity and high resistance to aggressive media (salts, low and high pH values) [3], [7], [9]. In the present work, the mechanism of acid corrosion of hardened GFPC paste system in nitric acid solutions have been studied in detail and compared to that of corresponding OPC system.

2 Experimental

2.1 Materials

Materials used for this work include ordinary Portland cement CEM-I 42.5 R and ordinary Portland cement clinker of the same. The chemical and mineralogical compositions are given in Table 1. The clinker was firstly pre-crushed in a jaw crusher, homogenized, and then the fraction under 7 mm was ground in a laboratory ball mill (23-liters capacity) in the presence of 0.05% (by weight of clinker) of a liquid grinding aid (ALSON TEA, a triethanolamine-based product from Chemotex company, Děčín-Boletice, Czech Republic). The grinding was continued until a Blaine specific surface area of 473 m^2/kg was attained.

Nitric acid was selected for the work. It is a highly corrosive mineral acid that is miscible with water in all proportions. Comparing to other strong acids like H_2SO_4 and HCl at equal pH values, the corrosive effect of nitric acid on cement based-materials is the most severe one [10], [11]. Pure nitric acid attack on cement-based materials can occur only in industrial environments.

2.2 Specimen preparation and test procedure

An aqueous solution was prepared by adding given amounts of sodium ligninsulphonate plasticizer and sodium carbonate to an amount of water for preparing a paste with a W/C of 0.22 that had an acceptable workability measured by flow-table. The solution was added to the ground clinker and the paste was formed into specimens of 20×20×20 mm in size. A number of OPC paste specimens of the same size were also prepared at a W/C of 0.30. All the specimens were kept in moulds at 95% relative humidity at 20°C for the first 24 hrs and then demoulded and stored in water at 20°C.

Table 1. Chemical and mineralogical phase compositions of OPC and OPC-clinker (wt%).

	OPC	OPC-Clinker
CaO	64.03	67.09
SiO_2	20.66	21.51
Al_2O_3	4.05	4.62
Fe_2O_3	2.59	2.35
MgO	2.19	1.79
SO_3	2.67	0.69
$K_2O + Na_2O$	0.97	1.11
LOI	0.50	-
C_3S	65.12	73.28
C_2S	10.10	6.39
C_3A	6.35	8.27
C_4AF	7.88	7.15

After 28 days, the specimens were immersed in three different solutions of nitric acid at pH values of 1±0.01, 2±0.03, and 3±0.05. All solutions were prepared by adding concentrated acids to tap water. The pH levels of the solutions were monitored daily with a portable pH-meter, and concentrated acids were added to maintain the pH values constant. During pH monitoring, an electrical mixer was used for mixing each of the solutions thoroughly. All the solutions were renewed monthly, and the temperature of the solutions was kept constantly at 20°C. The laboratory techniques used in this study include; X-ray diffractometry (XRD), scanning electron microscopy (JEOL), and electron-probe microanalysis (JEOL Superprobe 733).

3 Results and discussion

X-ray diffraction patterns of OPC and GFPC paste specimens after 28 days of curing are shown in Figure 1. The pattern of GFPC showing the presence of alite, belite, Portlandite, and calcium aluminate is very similar to that of OPC. The content of Portlandite in GFPC, however, is significantly reduced. The absence of Ettringite in GFPC implies a different hydration mechanism that is not yet understood.

According to Škvára [3], the main component of the binder product in hardened GFPC pastes is C-S-H (mean C/S ratio 2.7, based on EDAX analysis) inter-linked with very fine $Ca(OH)_2$ and highly dispersed C-A-H phases (hexagonal and cubic). The absence of crystalline formations, typical of hardened OPC paste, together with the high density and degree of dispersion of hydration products are responsible for the higher strength and durability attained in GFPC.

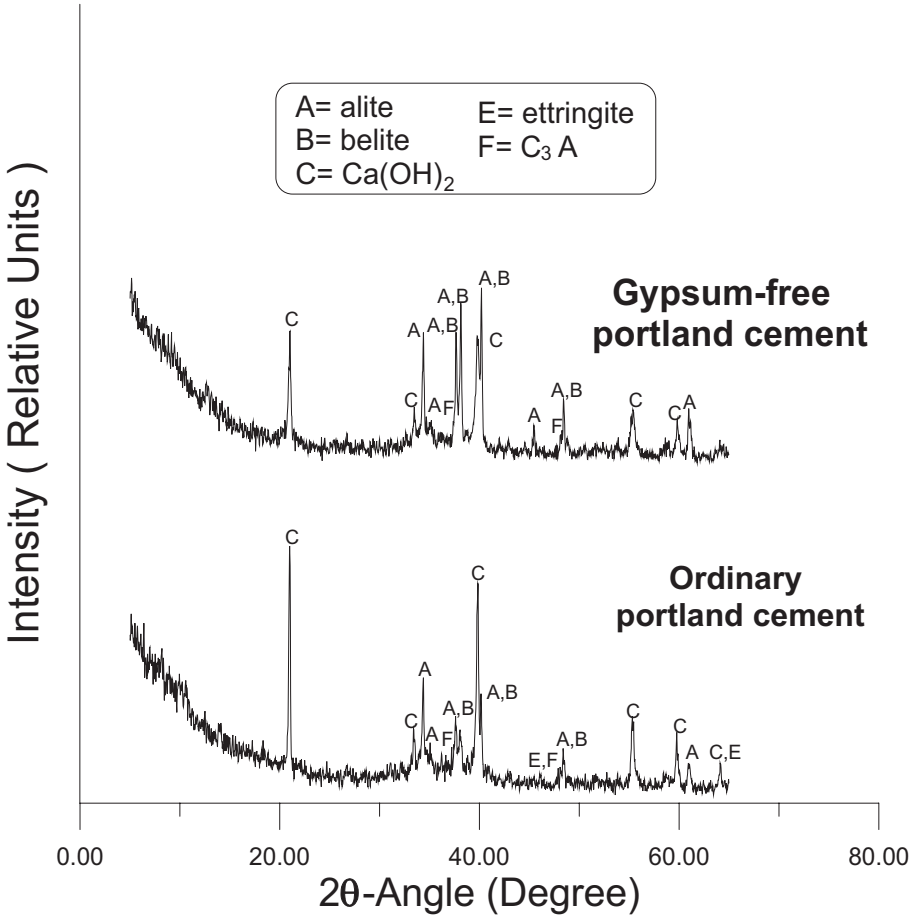

Fig. 1. X-ray diffraction patterns of OPC and GFPC pastes after 24 hrs in mould at 95% relative humidity at 20°C, followed by 27 days of curing in tap water at 20°C.

3.1 Visual observations

During corrosion, the changes in the appearance of the specimens were monitored visually. The observations are as follows:
At pH 1, the colour of the exposed surfaces gradually became lighter so that after 90 days of immersion, the developed corroded layer was white, extremely cracked, soft, and porous with no bonding properties. Upon drying in an open-air atmosphere, the corroded layer spalled off spontaneously. Visual observations for OPC specimens were the same, except for the colour and the size of shrinkage cracks which were slightly lighter and wider respectively.

At pH 2, the corroded layer which developed after 90 days of exposure was similar to that observed at pH 1, with the exception of a relatively thin brown zone adjacent to the uncorroded part. The brown colour of this internal zone was dark, and darker toward the boundary between the two parts. Careful inspection of the corroded specimens revealed that on the uncorroded side, adjacent to the corrosion zone, there existed a light-gray sub-layer. This sub-layer, which was slightly thinner than the external white corroded layer, was hard as a small section of the whole uncorroded part of the specimen. All the visual observations for OPC specimens were the same except the light gray sub-layer adjacent to the corrosion zone, which was nearly as thick as the corroded layer.

At pH 3, the corrosion process was so slow that, even after 90 days of immersion, the developed corroded layer was difficult to recognize. However, careful inspection showed that the colour of the acid-exposed surfaces had become slightly lighter compared to the uncorroded parts. Under drying, the gray colour of the acid-exposed surfaces changed to a very light brown and this made the corroded layer visually distinguishable.

3.2 Attack at pH 1

After 90 days of exposure to pH 1 nitric acid solution, a number of corroded GFPC and OPC specimens were removed and prepared for investigation by SEM. The areas observed under scanning electron microscope (Figures 2 - 5) were obtained by breaking specimens into halves to expose the total internal surface including the cross section of both corroded layers and uncorroded parts. Figure 2 shows typical microstructure of the uncorroded GFPC specimens. The unaffected microstructure of GFPC specimens was always found to be homogeneous and very dense (no or

very few visible porous regions) compared to that of OPC specimens. No crystalline structure like those typically found in hardened OPC (Portlandite crystals) can be seen in the compact microstructure of GFPC paste specimens.

Typical SEM micrographs of the microstructure of a corroded GFPC paste specimen at regions very close to the acid-exposed surface are shown in Figure 3. No distinct boundary was found between the corroded and uncorroded parts of the specimens, and the morphological appearance of the amorphous corrosion products deposited in the corroded layer was found to be more or less similar to that of unaffected phases in the sound inner parts. The extremely loose corroded layer,

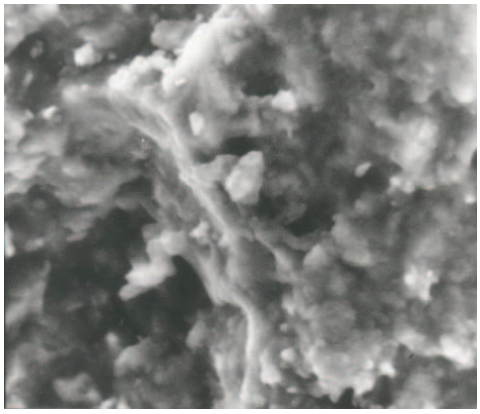

<–––––––––> 10 μm, 4000×

Fig. 2. Unaffected microstructure of GFPC paste specimen.

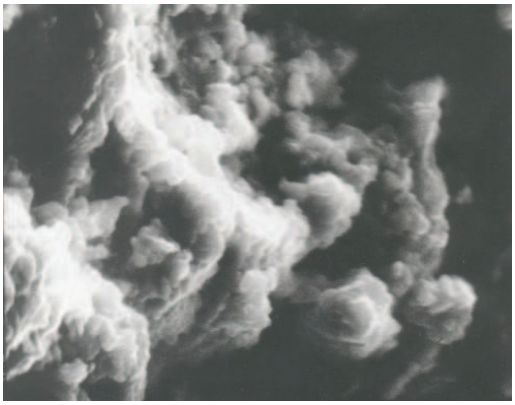

<–––––––––> 10 μm, 4000×

Fig. 3. Microstructure of a corroded GFPC paste specimen in a region very close to the acid exposed surface.

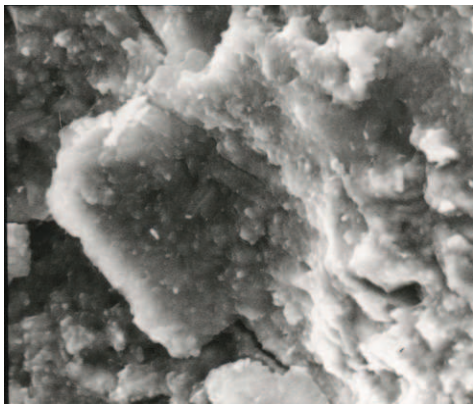

<–––––––––> 10 μm, 4000×

Fig. 4. Unaffected microstructure of OPC paste specimen.

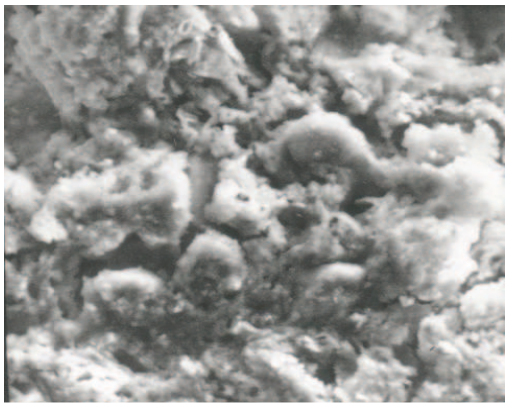

<––––> 10 μm, 2000×

Fig. 5. Microstructure of a corroded OPC paste specimen in a region very close to the acid exposed surface.

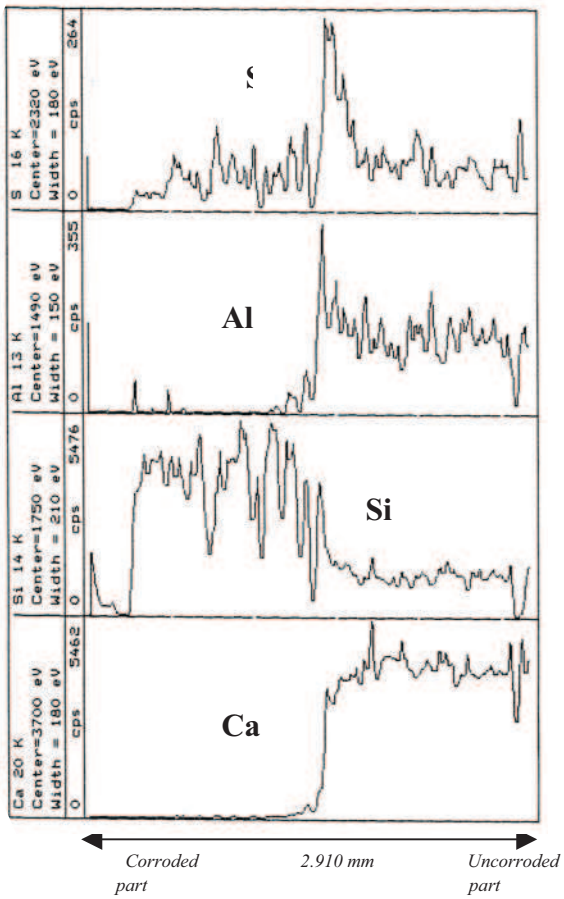

Fig. 6. X-ray line analysis (EDS) of a GFPC paste specimen, 90 days.

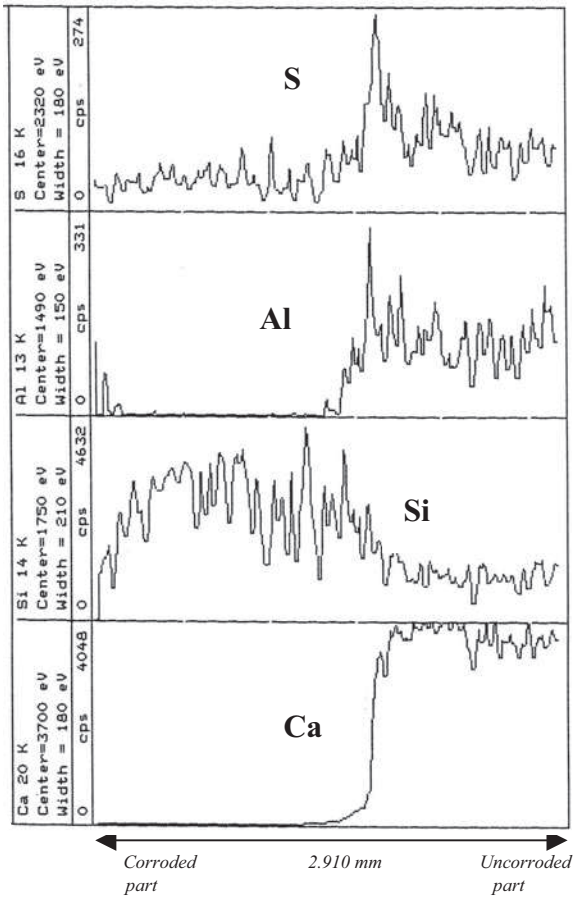

Fig. 7. X-ray line analysis (EDS) of a OPC paste specimen, 90 days.

however, can be distinguished from its highly increased pore content. Figures 4 and 5 show typical SEM micrographs of the microstructure of an attacked OPC paste specimen somewhere in the uncorroded part and at a region very close to the acid-exposed surface respectively. In the case of OPC specimens, the morphological appearance of the partially or completely corroded phases is quite different than that of intact phases present in the sound inner parts. In the partially corroded regions close to the corrosion zone, there was always evidence of calcium leaching along with a large number of shrinkage cracks.

A number of 90-day corroded specimens were also prepared for X-ray energy dispersion measurements. These measurements were performed across corrosion zones and along imaginary lines extending from somewhere in the corroded layers towards the internal unaffected parts of the specimens. The total length of line at a magnification of 40× is

2.910 mm. Typical results for GFPC and OPC specimens are presented in Figures 6 and 7 respectively. As seen in Figure 6, the corroded layer in GFPC specimens is mainly composed of hydrated silica, confirming that all the cement hydration products and unhydrated phases were completely decomposed and decalcified. Calcium concentration has abruptly decreased to zero due to the leaching of its highly soluble nitrate salt. The iron profile was not produced due to a problem in the EPMA instrument. Relative changes in the concentration of Fe however are expected to be similar to those of Al due to their relatively close solubility limits as reported by many authors [10]-[13]. A careful inspection of the profiles (Figure 6) shows that between the two main parts of the specimens there exists a thin sub-layer with markedly increased concentrations of Al and S. The concentrations of Ca and Si in this sub-layer respectively show slight decrease and increase, confirming that this sub-layer is the corrosion zone in which the cement hydration products and anhydrous phases have been partially corroded.

The presence of a relatively higher concentration of Al reveals that the pH value of the pore solution in this sub-layer is higher than the solubility limit of hydrated Al_2O_3. The pH value of the pore solution in this thin sub-layer, i.e. corrosion zone, therefore should follow a very steep gradient with a value close to 12.5 on the side of the uncorroded inner part to a much lower value less than the solubility limit of hydrated Al_2O_3 and close to that of acid solution, i.e. 1, on the other side. The significant increase in the concentration of S implies that the sulfate ions produced from the decomposition of sulfur-containing minerals of cement paste probably have a tendency to undergo a selective diffusion toward the counter-diffusing Ca^{2+} ions resulting in the formation of a gypsum deposit in the corrosion zone. However, it is difficult to prove the presence of gypsum, not only due to its very low concentration, but also due to the thickness of the corrosion zone (nearly 0.12 mm) making the sampling difficult.

3.3 Attack at pH 2

The results of X-ray energy dispersion measurements performed on 90-day corroded GFPC and OPC specimens are shown in Figures 8 and 9 respectively. The total length of line analysis at a magnification of 40× is 2.910 mm.

As seen in Figures 8 and 9, the corroded layers in both GFPC and OPC specimens are composed of a high concentration of hydrated SiO_2

along with a considerable amount of hydrated Al_2O_3 and a significantly decreased amount of Ca compared to the internal uncorroded parts. The concentration of Ca abruptly falls at the boundary between the two main parts and then steadily decreases to zero. This implies that dissolution of cement hydration products and anhydrous phases is taking place primarily in a relatively thin sub-layer, i.e. the main corrosion zone, at the boundary between the two main parts (similar to that observed at pH 1) and partially in a relatively thick sub-layer adjacent to the boundary on the corroded side.

The concentration of Al has an abrupt increase (enrichment) in the main corrosion zone, followed by a steady decrease to zero, showing that the hydrated Al_2O_3 produced from the decomposed cement phases firstly precipitates in the main corrosion zone and then slowly dissolves in a relatively thick sub-layer in the corroded part.

These observations confirm the presence of a gradient in pH value different than that expected for the case of attack at pH 1. The pH value of the pore solution therefore should follow a steep gradient in the main corrosion zone located at the boundary where Al shows an abrupt increase in concentration, followed by a gradual decrease to a much lower value less than the solubility limit of hydrated Al_2O_3 and close to that of acid solution, i.e. 2, across a relatively thick sub-layer in the corroded part.

The brown colour of the internal part of the corroded layer can be attributed to the accumulated ferric hydroxide. Pavlík [11], reporting a markedly increased amount of ferric oxide in the brown zone, stated that dissolution of ferric hydroxide at the outer side of this zone, where the pH value is lower than its solubility limit, results in an increase in the concentration of Fe^{3+} ions in the pore solution. The Fe^{3+} ions then diffuse not only out of the corroded layer into the aggressive solution, but also into the brown zone where at pH above 2 the ions again precipitate, resulting in an accumulation of hydrated iron oxide. Of further interest is the significant increase in the concentration of S, not only in the main corrosion zone at the boundary (as observed at pH 1), but also to a longer depth in the uncorroded side and, in particular, in the case of OPC specimen (Figure 9).

A careful inspection of the profiles shows that the concentration of Ca is slightly decreased in the same region. This is in fact the sub-layer visually distinguished from its light gray colour and reported by some authors [11], [14] for OPC paste specimens, the so-called ″core-layer ″. Pavlík [11] discusses the formation and properties of this sub-layer. No

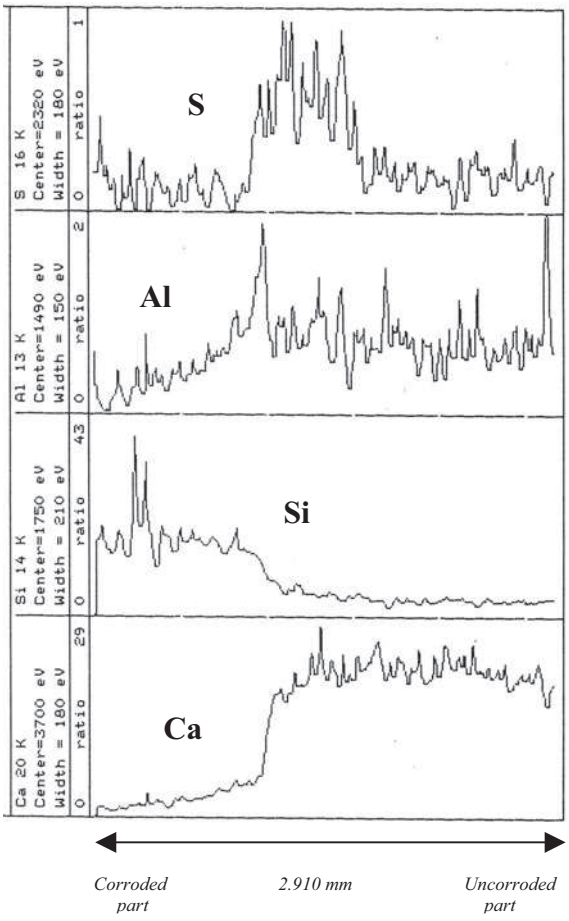

Fig. 8. X-ray line analysis (EDS) of GFPC paste specimen, 90 days corroded at pH 2 nitric acid solution.

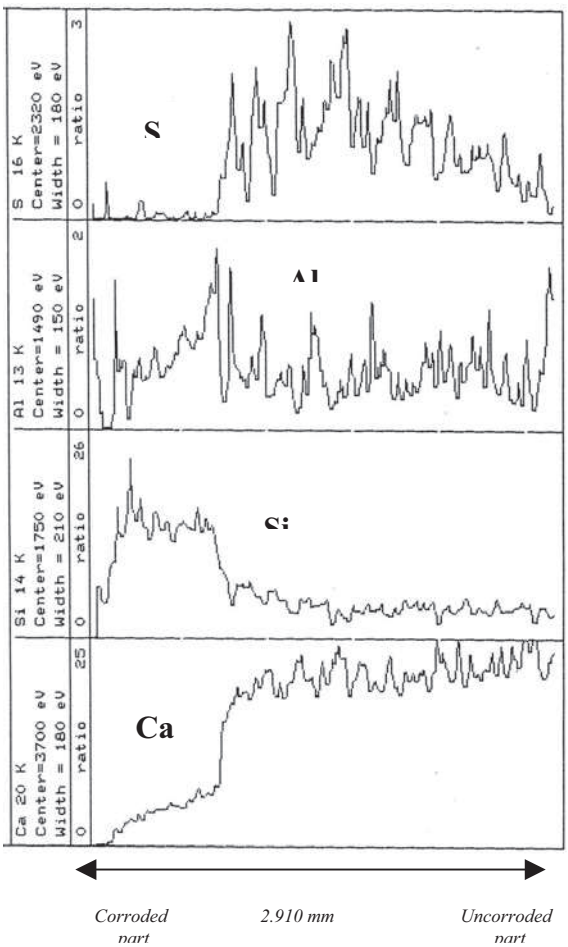

Fig. 9. X-ray line analysis (EDS) of OPC paste specimen, 90 days corroded at pH 2 nitric acid solution.

explanation has been given for the accumulation of S, probably caused by a selective diffusion of sulfate ions produced from the decomposed cement paste into this sub-layer.

Figure 10 shows the X-ray diffraction pattern of a sample of the above-mentioned core-layer, developed in GFPC paste specimens after 90 days of exposure to nitric acid solution at pH 2. The layer is composed of a relatively high content of calcite along with gypsum, ettringite, alite, and belite. Calcite is a secondary product, produced by a carbonation reaction with atmospheric CO_2 (the sample was prepared from corroded specimens stored in an open-air atmosphere for several months after removing the corroded layer). The presence of gypsum and ettringite, which were not originally present (refer to Figure 1), denotes that the significant increase in the sulfur content of the core-layer (refer to Figure 8) is due to the formation of gypsum and ettringite. The sulfate

ions produced from the decomposition of sulfur-containing minerals of the cement paste in the corrosion zone therefore undergo a selective diffusion across the corrosion zone and toward the uncorroded part. The sulfate ions therefore react with the counter-diffusing Ca^{2+} ions produced from dissolution of Portlandite and unhydrated calcium aluminate phase resulting in the formation of gypsum and ettringite.

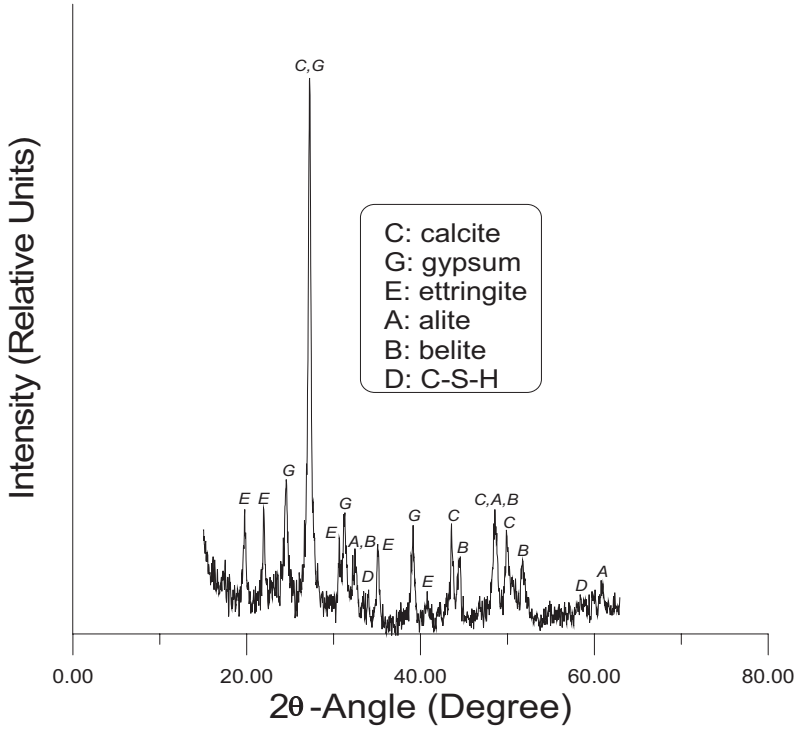

Fig. 10. X-ray diffraction pattern of the core-layer of GFPC paste specimen developed after 90 days of exposure to pH 2 nitric acid solution.

Formation of the core-layer confirms that nitric acid attack at relatively lower concentrations (pH≈2) not only commences in a relatively thin layer on the external surface, (i.e. the main corrosion zone, which gradually progresses inward), but also internally via inter-connected porosity. This is the conclusion previously made by Israel et al [14] for the case of attack by hydrochloric and ethanoic acids. As Pavlík [11] stated, formation of the core-layer is noticeable only for lower concentrations and relatively longer exposure times. At higher concentrations (pH≈1), however, the corrosion process is limited to a very thin corrosion zone which progresses inward at a comparatively higher velocity.

3.4 Attack at pH 3

Figures 11 and 12 represent the concentration profiles obtained from X-ray energy dispersion measurements performed on specimens of GFPC and OPC after an exposure period of 90 days to nitric acid solution at pH 3 respectively. The total length of line analysis at a magnification of 40× is 1.164 mm. The exact similarity between the corresponding concentration profiles reveals that at relatively high pH values of nitric acid solution the same corrosion mechanism is also at work for hardened pastes of both GFPC and OPC.

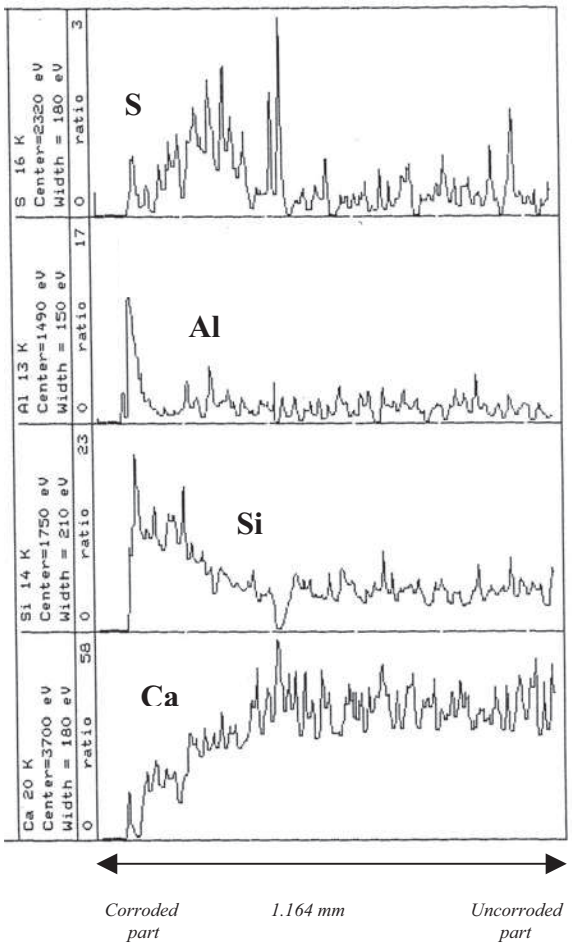

Fig. 11. X-ray line analysis (EDS) of GFPC paste specimen, 90 days corroded at pH 3 nitric acid solution.

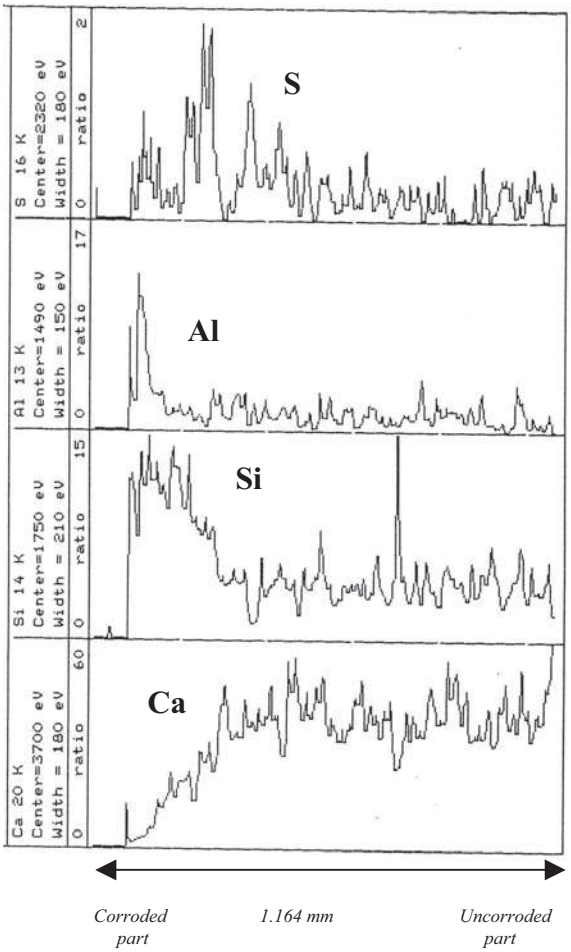

Fig. 12. X-ray line analysis (EDS) of OPC paste specimen, 90 days corroded at pH 3 nitric acid solution.

The affected layers, as seen, show a steady increase in the concentration of Si, revealing a gradual dissolution of cement paste. The concentration of Ca steadily decreases to near zero in regions very close to the acid-exposed surface where Al shows an abrupt increase in concentration. Such an abrupt increase in Al concentration, and only in a relatively thin sub-layer at the outermost part of the affected layer, implies that the Al-containing hydrates and/or phases are likely the last dissolving compounds. Formation of the core-layer is not significant, probably due to the relatively short exposure time.

3.5 Extent of corrosion

After 28 days of curing, a number of paste specimens were used to compare the extent of corrosion. The exact size of each specimen from the face to be exposed to the acid solution to the opposite one was first measured by a caliper with an accuracy of 0.02 mm. The specimens were then prepared for establishing a unidirectional corrosion process by covering all the faces, except the one to be exposed, with a thin layer of grease. The specimens were then immersed in the acid solutions. The ratio of solution volume (cm^3) to the total corrosion surface (cm^2) was kept constant at 50.

During the course of corrosion and at different time intervals, specimens were removed from the acid solutions and after completely removing the corrosion residuals by brushing with a steel-wire brush, the corrosion depths of different binders were determined by accurately measuring the uncorroded parts of the specimens using the caliper and subtracting the values from their accurately measured initial sizes. For each measurement of corrosion depth two specimens were used and the average of the two measurements was reported. The precision and accuracy of the measurements was about 0.02 mm. The results are presented in table 1. As seen, the extent of corrosion decreases considerably in the case GFPC. The relatively higher acid resistance of GFPC can be attributed to the absence of crystalline formations, typical of hardened OPC paste, together with the high density and degree of dispersion of hydration products in its hardened paste.

Table 2. Corrosion depths (mm) in nitric acid solutions.

Exposure Time (day)	pH 1		pH 2		pH 3	
	OPC	GFPC	OPC	GFPC	OPC	GFPC
0	0	0	0	0	0	0
4	1.32	0.90	0.30	0.10	-	-
10	1.98	1.65	0.40	0.32	-	-
30	4.13	3.23	0.72	0.62	-	-
50	5.34	4.32	1.00	0.90	-	-
60	-	-	-	-	0.31	0.24
70	6.92	5.30	1.39	1.15	0.32	0.28
80	-	-	-	-	0.37	0.31
90	8.16	6.56	1.62	1.40	0.40	0.33

4 Conclusion

Hardened paste of gypsum-free Portland cement is corroded by exactly the same mechanism as hardened paste of ordinary Portland cement. The only difference between the two types of cement is the rate of corrosion. The absence of crystalline formations, typical of hardened OPC paste, together with the high density and degree of dispersion of hydration products are responsible for a relatively higher acid resistance in GFPC.

References

[1] Allahverdi A. and Škvára F., "Acidic Corrosion of Hydrated Cement Based Materials, Part 1; Mechanism of the Phenomenon", Ceramics-Silikáty, 44(3), 114-120, 2000.

[2] Allahverdi A. and Škvára F., "Acidic Corrosion of Hydrated Cement Based Materials, Part 2; Kinetics of the Phenomenon and Mathematical Models", Ceramics-Silikáty, 44(4), 121-160, 2000.

[3] Škvára F., "Gypsum-free Portland Cement Pastes of Low Water-to-Cement Ratio", Mater. Res. Soc. Symp., 370, 153-158, 1995.

[4] Škvára F., "Properties of Gypsum-free Portland Cement Pastes with a Low Water-to-Cement Ratio", Ceramics-Silikáty, 40(1), 36-40,1996.

[5] Hrazdirs J., "The Properties of Gypsum-free Portland Cements with an Admixture of ABESON-TEA Grinding Aid", Ceramics-Silikáty, 36(2), 87-91, 1992.

[6] Škvára F., "The Effects of the Mineralogical Composition of Clinker on the Properties of Gypsum-free Portland Cements", Ceramics-Silikáty, 37(4), 181-184, 1993.

[7] Škvára F., "Corrosion of Low Porosity Materials Prepared with the Use of Alkali-activated Gypsum-free Portland Cement" Alkaline Cem. and Conc., Proc. Int. Conf. 2nd, Kyiev, Ukraine, 44-50, 1999.

[8] Škvára F. and Ševčik V., "Influence of High Temperature on Gypsum-free Portland Materials", Cem. Concr. Res. 29, 713-717, 1999.

[9] Škvára F., "Corrosion of Low-porosity Materials Prepared with the Use of Gypsum-free Portland Cement", Ceramic-Silikáty, 38(3, 4), 159-162, 1994.

[10] Pavlík V., "Corrosion of Hardened Cement Paste by Acetic and Nitric Acids, Part I: Calculation of Corrosion depth", Cem. Conc. Res., 24(3), 551-562, 1994.

[11] Pavlík V., "Corrosion of Hardened Cement Paste by Acetic and Nitric Acids, Part II: Formation and Chemical Composition of the Corrosion Products Layer", Cem. Conc. Res., 24(8), 1495-1508, 1994.

[12] Chandra S., "Hydrochloric Acid Attack on Cement Mortar – An Analytical Study", Cem. Conc. Res., 18(2), 193-203, 1988.

[13] De Ceukelaire L.," The effects of Hydrochloric Acid on Mortar", Cem. Conc. Res., 22, 903-914, 1992.

[14] Israel D. and Macphee D.E., "Acid Attack on Pore-reduced Cements", J. Mater. Sci., 32, 4109-4116, 1997.

Ali Allahverdi, PhD
Institute: College of Chemical Engineering,
Iran University of Science and Technology
Narmak 16846, Tehran, Iran
Phone/Fax: (+98)09123838714,
(+98)2177240495
E-mail: ali.allahverdi@iust.ac.ir